

Cathodoluminescence Quenching in Yb-doped ZnO Nanostructures

A. Susarrey-Arce¹, M. Herrera-Zaldívar^{1,a}, W. de la Cruz¹, and U. Pal²

¹Centro de Ciencias de la Materia Condensada, Universidad Nacional Autónoma de México, Apdo. Postal 2681, Ensenada, BC 22800, Mexico

²Instituto de Física, Universidad Autónoma de Puebla, Apdo. Postal J-48 Puebla, Pue. 72570, Mexico

^azaldivar@ccmc.unam.mx (corresponding author), Fax: +52-646-1744603

Received: July 20th, 2007, revised: January 30th, 2008, accepted: February 20th, 2008

Keywords: ZnO nanostructures, Yb-doping, Cathodoluminescence,

Abstract. Cathodoluminescence (CL) quenching was observed in ZnO nanostructures when doped with Yb by both chemical and physical methods. CL spectra of the samples revealed a defect emission at 2.25 eV in samples prepared by the chemical method, and an emission at 2.5 eV in samples prepared by the physical method. From the thermal treatment studies, it was found that oxygen vacancies are responsible for the 2.5 eV emission. Observed CL quenching in ZnO is explained through the participation of point defects in the energy transfer process from ZnO to Yb³⁺.

Introduction

Recently, semiconductor nanostructures have generated a great interest because they afford an ability to control defect states by changing the particle shapes and sizes. Luminescence properties of ZnO nanostructures have been extensively studied in the last several years keeping in mind their applications as field emitters and light emitting devices [1,2]. While the large exciton binding energy (60 meV) of ZnO facilitates the gain mechanism of such devices, the relatively easy synthesis of ZnO in nanostructure forms is the other reason for the enhanced interest in the study of its optical properties. Studies of the incorporation of rare earth (RE) ions in ZnO nanostructures have been reported recently [3-6]. The RE ions produce sharp and intense emission lines due their 4f intrashell electronic transitions. The luminescence properties of the RE ions depends on the band gap energy of the host semiconductor [7], and on the symmetry center occupied by the RE ion in the host [8,9]. Although, Yb³⁺ ions have been successfully incorporated in other semiconductors such as GaN [10,11], which possess similar crystallographic and optical properties to ZnO, there are very few reports related to incorporation of Yb³⁺ in ZnO. Recently U. Pal *et al.* [6] have reported a thermoluminescence study of ZnO:Yb nanophosphors exposed to beta radiation. They have shown that these materials exhibit low thermoluminescence fading due to the presence of electronic trap states. Defects in semiconductors introduce trap states, which can affect the optical activation of the RE by energy absorption [12,13]. However, in a slow energy transfer process such as from ZnO host to Eu³⁺, some defects apparently participate as storage centers to transfer the energy at long time periods [5].

In the present work, cathodoluminescence (CL) microscopy and spectroscopy are used to investigate the effect of Yb doping on the defect structures in ZnO nanostructures. Effect of Yb doping through chemical and physical processes in ZnO nanostructures on their CL emissions are studied. Participation of defects in the energy transfer process from the ZnO host to Yb is discussed.

Experimental

For the chemical doping, ZnO nanostructures were grown by a glycol mediated chemical synthesis. In a typical synthesis process, 0.025M of anhydrous zinc acetate $[(C_2H_3O_2)_2Zn]$, Aldrich, 99.99% was added to 1M of ethyleneglycol (Baker) in a round bottom flux and heated at 440 K temperature for 2 h. After cooling to room temperature (RT), the white mixture was filtered and washed by ethanol and water repeatedly and dried at RT. For Yb doping, $YbCl_3 \cdot 6H_2O$ (Alfa Aesar, 99.9%) of 1 and 5 mol % (nominal) was added to the reaction mixture before heating.

For physical doping, ZnO powder (Alfa-Aesar 99.9%) was mixed with nominal 2 and 10 mol % of $YbCl_3 \cdot 6H_2O$ (Alfa Aesar, 99.9 %) and ground in an agate mortar; followed by thermal annealing at 150 °C in Ar atmosphere for 5 h. Finally, the samples were washed with distilled water.

All the samples were analyzed by energy dispersive spectroscopy (EDS), secondary electron and CL modes of SEM, and CL spectroscopy, using a Jeol JSM 5300 scanning electron microscope (SEM). For CL-SEM analysis of the samples, electron beam energy of 15 keV and beam current of 27 nA were used. CL measurements were performed at sample temperature of 100 K in the UV-visible spectral range, using a Hamamatsu R928P photomultiplier. A SPEX 340-E computer-controlled monochromator was used for spectral analysis.

Composition of the samples was studied by x-ray photoelectron spectroscopy (XPS), using a non-monochromatic Al K_{α} x-ray line (1486.6 eV) of SAM-PHI 548 system. The energy scale was pre-calibrated using the reference binding energies of Cu $2p_{3/2}$ (932.67 eV), and Ag $3d_{5/2}$ (368.26 eV) lines.

Results

Secondary electron images of the chemically prepared samples reveal the formation of spherical particles of diameters between 200 and 1000 nm [Fig. 1(a)]. Incorporation of Yb affected negatively the size and shape control of the particles. Formation of some bigger clusters in Yb doped samples, apparently by the agglomeration of smaller nanoparticles can be seen in the inset of Fig 1(b). In general, the average particle size of the glycol-mediated ZnO nanoparticles decreased a bit on Yb doping. The Yb contents in doped samples estimated by EDS (not presented) were about 0.5 and 0.8 atom %, respectively.

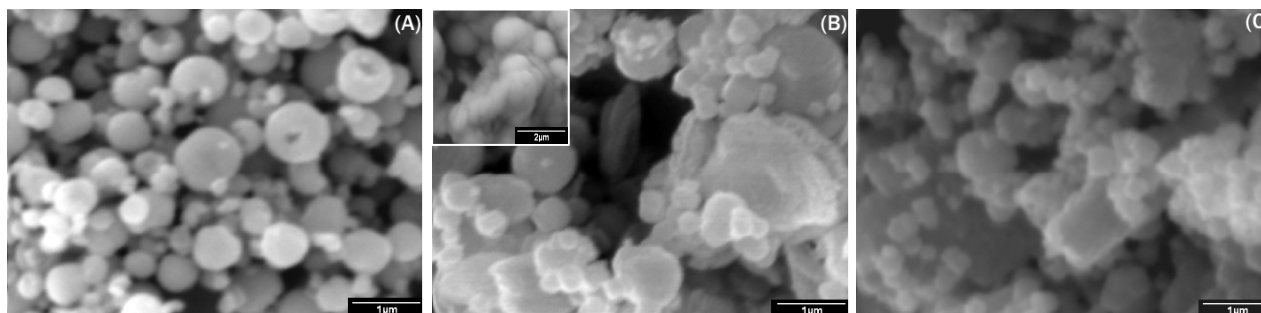


Figure 1. SEM images of ZnO nanoparticles synthesized by the chemical method: (a) undoped, (b) 2% Yb doped, and (c) 5% Yb doped.

CL spectra of the chemically synthesized nanostructures revealed 3.21 and 2.25 eV emission bands, which correspond to the near band edge emission and defect related yellow emission in ZnO (Fig. 2). The relative intensities of the emission bands, I_{UV}/I_{yellow} , were about 11.7, 5.8, and 0.9 for the undoped, 1% Yb doped and 5% Yb doped samples, respectively. A quenching of the near band edge emission on incorporation of Yb can be noticed, which is more evident 5% Yb doped sample. A slight increase of the yellow emission intensity was observed for the 5% Yb doped sample. CL

images show an inhomogeneous luminescence distribution for all the samples (Fig. 3). While the undoped ZnO exhibits intense CL emission from the nanoparticles [Fig. 3(a) and (b)], Yb doped samples exhibit low emissions from smaller nanoparticles and high emission from bigger ones [Fig 3(e) and (f)].

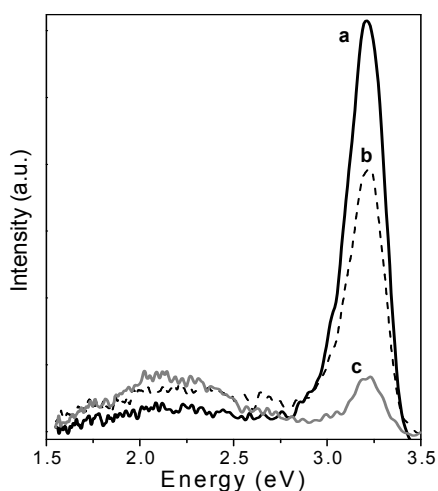
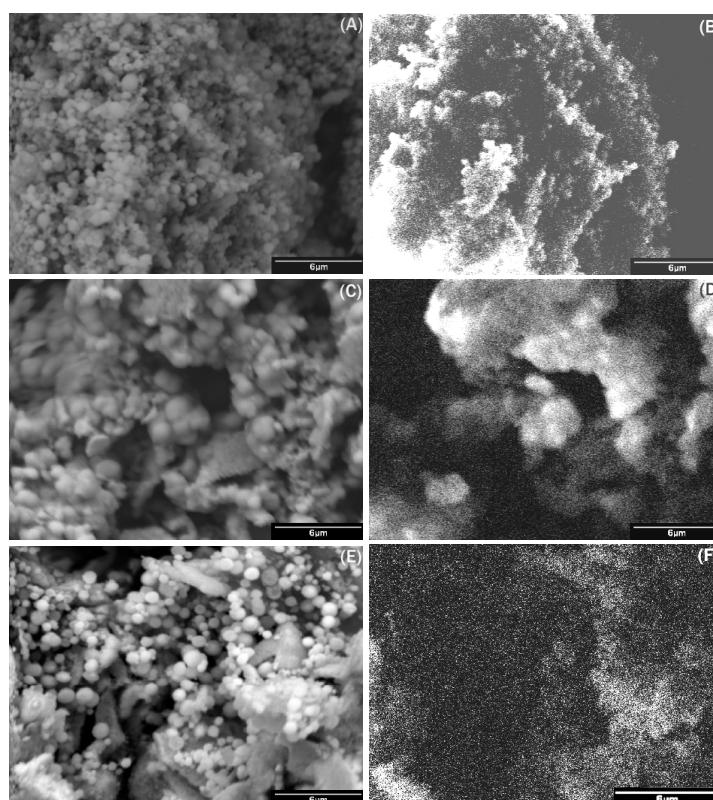


Figure 2. CL spectra of ZnO nanoparticles doped with different Yb contents: (a) undoped, (b) 2% Yb doped, and (c) 5% Yb doped.

During physical preparation, XRD spectra were acquired at different steps to monitor the formation of other compounds beside ZnO. After grinding pure ZnO with $\text{YbCl}_3 \cdot 6\text{H}_2\text{O}$ and before thermal treatment, there appeared no XRD peak related to YbCl_3 (spectrum c, Fig. 4). However, there appeared several weak peaks superimposed on the ZnO spectrum (indicated by arrows in the spectrum c), which were not identified. Presence of chlorate compounds in the annealed samples was revealed by XPS measurements (discussed below). After thermal treatment of the doped samples, their XRD spectra revealed only peaks related to ZnO (spectra d and e, Fig. 4).

Figure 3. SEM and corresponding panchromatic CL images of chemically prepared ZnO nanoparticles: (a-b) undoped, (c-d) 1% Yb doped, and (e-f) 5% Yb doped.



CL spectrum of pure ZnO show emission bands at around 3.16 and 2.5 eV, which correspond to the band edge emission and the well know defect related green emission [curve 1 in

Fig. 5(a)] of ZnO, respectively. On grinding the pure ZnO, the CL spectrum revealed a red-shift of band edge emission along with a drastic reduction of defect emission intensity [curve 2 in Fig. 5(a)]. This last effect was also observed for the pure ZnO sample after annealing at 700 °C for 5 h, although with a small blue-shift of band edge emission as shown as the curve 3 in Fig. 5(a).

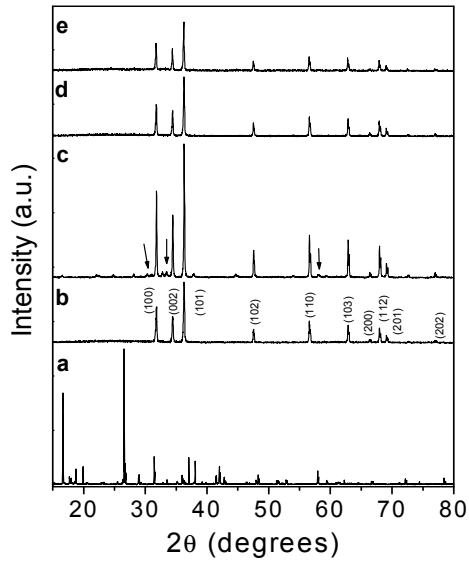


Figure 4. XRD spectra of (a) $\text{YbCl}_3 \cdot 6\text{H}_2\text{O}$, (b) undoped ZnO, (c) 10% Yb doped ZnO before thermal annealing; (d) 2% Yb doped and (e) 10% Yb doped ZnO annealed in Ar at 150 °C by 5 h.

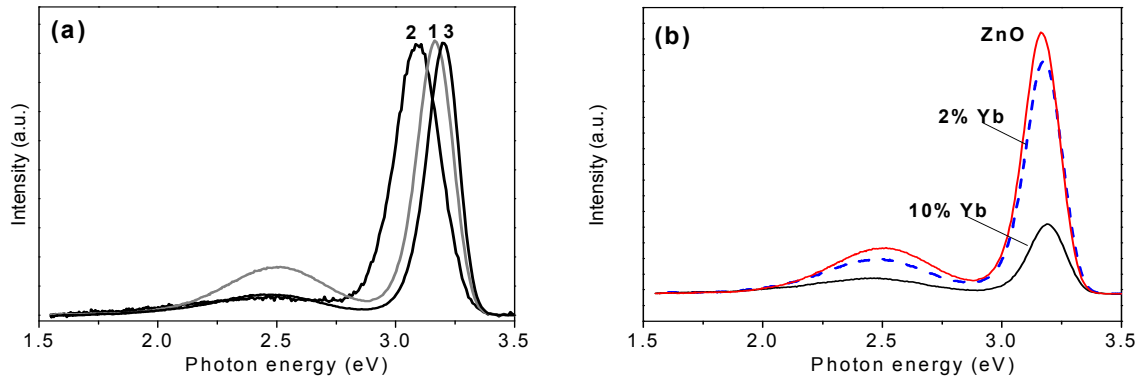


Figure 5. (a) Normalized CL spectra of undoped ZnO (curve 1), undoped ZnO grinded (curve 2) and ZnO annealed in O_2 atmosphere at 700 °C (curve 3). (b) CL spectra of undoped, 2% Yb doped, and 10% Yb doped ZnO, after annealing at 150 °C in Ar.

CL spectra of the Yb doped and annealed ZnO samples revealed the quenching of the green emission along with the reduction of band edge emission intensity [Fig. 5(b)], in analogy with the samples prepared chemically. In physically prepared samples, however, a blue-shift of band edge emission from 3.16 to 3.19 eV occurs during the Yb incorporation process. The CL images revealed a similar CL contrast (distribution of bright and dark particles) for the pure and Yb doped ZnO samples (Fig. 6).

Figure 6. Typical (a) SEM and (b) panchromatic CL image of ZnO nanostructures doped with 10% Yb through physical method.

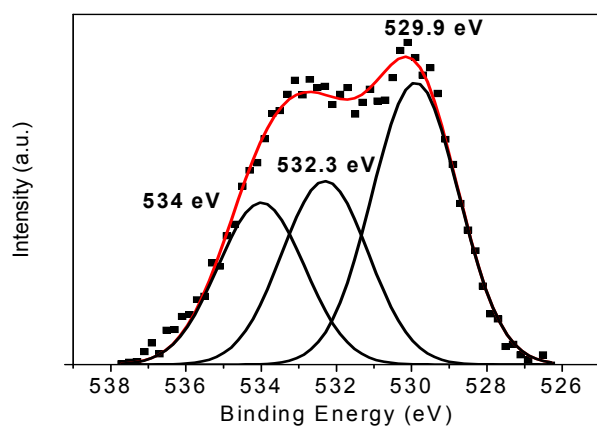
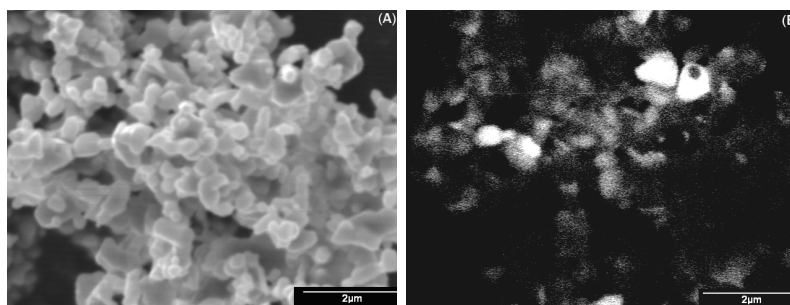


Figure 7. Deconvoluted oxygen peak in the XPS spectrum of physically prepared and annealed 10% Yb doped ZnO, showing three components at 529.9, 532.3, and 534 eV, which correspond to ZnO, $(\text{ClO}_3)^-$ ions and CO_2 , respectively.

XPS measurements on the sample doped with 10% Yb revealed about 4.0, 43.0, 45.1, and 7.8 at % of Yb, Zn, O and Cl, respectively. High resolution XPS measurements on the oxygen signal recorded a component centered around 532.3 eV (Fig. 7), which suggest the presence of chlorate ions $[(\text{ClO}_3)^-]$ in the doped samples after thermal treatment.

Discussion

The ZnO samples studied here contain different structural defects, as revealed from their CL spectra. The chemically prepared samples show a weak yellow emission, which increases with the increase of Yb content (Fig. 2). This emission has been related to the oxygen interstitial type point defects in ZnO [14]. CL spectra of physically Yb doped ZnO revealed the presence of the well known green emission (2.5 eV), which has been assigned to the point defects originating mainly from oxygen vacancies (V_O) [15]. Quenching of the green emission in undoped ZnO either by thermal annealing in oxygen or by mechanically grinding in air is due to incorporation of oxygen and reduction of V_O [Fig. 5(a)]. Analogously, suppression of V_O in ZnO is expected by the milling with YbCl_3 , although incorporation of oxygen in the mixture apparently produce chlorates compounds such revealed the XPS measurements (Fig. 7).

Our results show that the CL emissions of ZnO nanostructures quench on Yb incorporation, either by physical or by chemical method. Similar effect has been observed in Yb doped GaAs [16] and GaSb [17], where, apparently the deep electron traps affect the energy transfer process from the host to Yb^{3+} . However, in ZnO, it has been observed that the quenching of their luminescence by the incorporation of Eu^{3+} is due to activation of RE ions through an energy transfer process from ZnO host [18]. In general, the energy transfer from ZnO to the rare earth ions is small. As has been explained by Jia *et al.* [5], since the lifetime of excitons is very short (\sim several hundred picoseconds), and the energy transfer rate to the rare earth is of 10^7 per second, not much energy can be absorbed by the rare earth ions during exciton recombinations. They have proposed that the energy transfer from ZnO to Eu^{3+} increases by the participation of defects, which apparently act as

energy storage centers, permitting the energy to be transferred to the RE ions in a reasonably long time period. The possible participation of the defects in the energy transfer to the Yb^{3+} in the samples prepared chemically is not very clear. An integral CL quenching of the ZnO is expected in the energy transfer process, as occurred in the Yb doped samples prepared physically. While the green emission originating principally from oxygen vacancies, has a short lifetime of about 200 ps [19], the yellow emission present a long lifetime [20]. As reported by Kahn *et al.* [21], in ZnO nanoparticles of 4 nm, the yellow emission life time is about 1850 ns. While the defects related with the yellow emission present longer lifetime, and could participate as energy storage centers and transfer energy to the Yb^{3+} slowly; instead of quenching, the intensity of this emission increased on Yb doping for the chemically prepared sample (Fig. 2). On the other hand, although the defects related to the green emission (in mechanically prepared samples) could participate in the energy transfer process, a low efficiency process is expected since their lifetime is similar to the lifetime of excitons in ZnO. In general, weak energy transfer implies weak interaction between the conduction electrons and doping ions. As the lifetime of excitons in ZnO is very short (\sim hundreds of picoseconds), and the energy transfer rate for rare earths is $\sim 10^7$ per second [5], most of the energy will be released through other channels before the excitation energy transfer from the host to the doping ions. Moreover, we could not detect the emission related to Yb^{3+} interband transition ${}^2\text{F}_{7/2} \rightarrow {}^2\text{F}_{5/2}$ (at about 1000 nm) [11] in our samples using a Si photodiode as detector. While some energy storage centers can be created in ZnO by Yb doping, Yb^{3+} possibly will bring more anions into the host lattice, reducing the concentration of oxygen vacancies, and hence reducing the green emission. Therefore, the Yb doping in ZnO forms deep electron traps in the band gap, which do not favor the transfer of energy to excite Yb^{3+} ions, but capture electrons from the shallow donor levels close to the conduction band.

Conclusions

Quenching of integrated CL intensity occurred in ZnO nanostructures upon doping with Yb either by physical or by chemical methods. While the yellow emission at about 2.25 eV related to oxygen interstitial type point defects was the dominant defect band in the chemically prepared ZnO nanostructures, oxygen vacancy-related green emission at about 2.5 eV was the main defect band in physically prepared ZnO nanostructures. Participation of the point defects in the energy transfer process from ZnO to RE ions apparently can not explain the observed quenching of CL emissions in ZnO nanostructures. Incorporation of Yb^{3+} into the ZnO lattice possibly reduces the concentration of oxygen vacancies, causing a reduction of the green emission. Quenching of integrated CL intensity in Yb doped ZnO nanostructures is due to the formation of deep electron traps in the band gap which capture electrons from the shallow donor levels close to the conduction band.

Acknowledgments

This work was supported by CONACyT, DGAPA-UNAM, and UC-MEXUS through grants # 47505 & 46269, # IN120506 and # CN-05-215, respectively. ASA thanks CONACyT for the doctoral fellowship. Technical helps of E. Flores, E. Aparicio, V. García, I. Gradilla and A. Pérez are also acknowledged.

References

[1] Z. Z. Zhang, Z. P. Wei, Y. M. Lu, D. Z. Shen, B. Yao, B. H. Li, D. X. Zhao, J. Y. Zhang, X. W. Fan, and Z. K. Tang: *J. Cryst. Growth* Vol. 301 (2007), p. 362

- [2] Z. P. Wei, Y. M. Lu, D. Z. Shen, Z. Z. Zhang, B. Yao, B. H. Li, J. Y. Zhang, D. X. Zhao, and X. W. Fan, and Z. K. Tang: *Appl. Phys. Lett.* Vol. 90 (2007), p. 42113
- [3] S. Sadhu, T. Sen, and A. Patra: *Chem. Phys. Lett.* Vol. 440 (2007), p. 121
- [4] A. Ishizumi and Y. Kanemitsu: *Appl. Phys. Lett.* Vol. 86 (2005), p. 253106
- [5] W. Jia, K. Monge, and F. Fernández: *Opt. Mater.* Vol. 23 (2003), p. 27
- [6] U. Pal, R. Meléndez, V. Chernov, and M. Barboza-Flores: *Appl. Phys. Lett.* Vol. 89 (2006), p. 183118
- [7] P. N. Favennec, H. L'Haridon, S. Salvi, D. Moutonnel, and Y.L. Guillou: *Electron. Lett.* Vol. 25 (1989), p. 718
- [8] T. Monteiro, C. Boemare, M. J. Soares, R. A. Sá Ferreira, L. D. Carlos, K. Lorenz, R. Vianden, and E. Alves: *Physica B* Vol. 308 (2001), p. 22
- [9] J. B. Gruber, B. Zandi, H. J. Lozykowski, and W. M. Jadwisienczak: *J. Appl. Phys.* Vol. 92 (2002), p. 5127
- [10] M. Dammak, S. Kammoun, R. Maalej, and M. Kamoun: *J. Alloys and Compd.* Vol. 432 (2007), p. 18
- [11] W. M. Jadwisienczak and H. J. Lozykowski: *Opt. Mater.* Vol. 23 (2003), p. 175
- [12] T. Monteiro, A.J. Neves, M.C. Carmo, M.J. Soares, M. Peres, E. Alves, E. Rita, and U. Wahl: *Superlattices Microstruct.* Vol. 39 (2006), p. 202
- [13] S. Kim, S. J. Rhee, D. A. Turnbull, E.E. Reuter, X. Li, J.J. Coleman, and S.G. Bishop: *Appl. Phys. Lett.* Vol. 71 (1997), p. 231.
- [14] K. L. Wu, G.G. Siu, C. L. Fu, and H. C. Ong: *Appl. Phys. Lett.* Vol. 78 (2001), p. 2285
- [15] F. Leiter, H. Alves, D. Pfisterer, N.G. Romanov, D.M. Hofmann, and B.K. Meyer: *Physica B* Vol. 340 (2003), p. 201
- [16] A. Taguchi, H. Nakagomeand, and K. Takaheid: *J. Appl. Phys.* Vol. 68 (1990), p. 3390
- [17] P. Hidalgo, B. Mendez, C. Ruiz, V. Bermudez, J. Piqueras, and E. Diéguez: *Mater. Sci. Eng., B* Vol. 121 (2005), p. 108
- [18] Y. K. Park, J. I. Han, M. G. Kwak, H. Yang, S. H. Ju, and W.S. Cho: *J. Lumin.* Vol. 78 (1998), p. 87
- [19] B. Guo, Z. R. Qiu, and K. S. Wong: *Appl. Phys. Lett.* Vol. 82 (2003), p. 2290
- [20] O. F. Schirmer and D. Zwingel: *Solid State Commun.* Vol. 8 (1970), p. 1559
- [21] M. L. Kahn, T. Cardinal, B. Bousquet, M. Monge, V. Jubera, and B. Chaudret: *Chem. Phys. Chem.* Vol. 7 (2006), p. 2392

Journal of Nano Research Vol. 5

doi:10.4028/0-00000-029-9

Cathodoluminescence Quenching in Yb-Doped ZnO Nanostructures

doi:10.4028/0-00000-029-9.177